MOLECULAR ECOLOGY

Molecular Ecology (2011) **20**, 3989–4008 doi: 10.1111/j.1365-294X.2011.05248.x

Bayesian inference of a historical bottleneck in a heavily exploited marine mammal

J. I. HOFFMAN,* S. M. GRANT,† J. FORCADA† and C. D. PHILLIPS‡

**Department of Animal Behaviour, University of Bielefeld, Postfach 100131, 33501 Bielefeld, Germany, †British Antarctic Survey, Natural Environment Research Council, High Cross, Madingley Road, Cambridge CB3 0ET, UK, ‡Department of Biological Sciences, Texas Tech University, Lubbock, Texas 79409, USA*

Abstract

Emerging Bayesian analytical approaches offer increasingly sophisticated means of reconstructing historical population dynamics from genetic data, but have been little applied to scenarios involving demographic bottlenecks. Consequently, we analysed a large mitochondrial and microsatellite dataset from the Antarctic fur seal *Arctocephalus gazella*, a species subjected to one of the most extreme examples of uncontrolled exploitation in history when it was reduced to the brink of extinction by the sealing industry during the late eighteenth and nineteenth centuries. Classical bottleneck tests, which exploit the fact that rare alleles are rapidly lost during demographic reduction, yielded ambiguous results. In contrast, a strong signal of recent demographic decline was detected using both Bayesian skyline plots and Approximate Bayesian Computation, the latter also allowing derivation of posterior parameter estimates that were remarkably consistent with historical observations. This was achieved using only contemporary samples, further emphasizing the potential of Bayesian approaches to address important problems in conservation and evolutionary biology.

Keywords: Antarctic fur seal, Approximate Bayesian Computation (ABC), Bayesian Skyline Plot (BSP), bottleneck, conservation genetics, demographic history, heterozygosity excess, microsatellite, mtDNA, pinniped

Received 27 April 2011; revision received 11 July 2011; accepted 20 July 2011

Introduction

Many natural populations have experienced severe demographic reductions, or population bottlenecks, due to over-exploitation or anthropogenically induced habitat destruction. This is a major cause of concern to conservation biologists because bottlenecks can lead to the loss of genetic variability, elevated levels of inbreeding and the fixation of mildly deleterious alleles, thereby increasing the risk of extinction and compromising adaptive evolutionary potential (Hedrick & Miller 1992; Lande 1994; Mills & Smouse 1994; Lynch *et al.* 1995; Frankham *et al.* 1999). Unfortunately however, detecting and measuring the impacts of such changes is not usually possible because patterns of historical abundance are seldom known. Consequently, there has been considerable interest in the development and application of methods for detecting bottleneck signatures using neutral genetic markers such as microsatellites.

One such approach exploits the fact that genetic drift is intensified in small populations, leading to concomitant changes in allele frequencies and in some cases the fixation or loss of alleles. This in principle allows changes in the effective population size to be measured when multiple, temporally spaced samples are available (Waples 1989; Luikart *et al.* 1999; Williamson & Slatkin 1999; Anderson *et al.* 2000; Beaumont 2003). However, this approach may underestimate the magnitude of severe bottlenecks because the loss of alleles constrains the extent to which allele frequencies are subsequently able to drift (Richards & Leberg 1996). Perhaps more importantly, to detect a historical reduction in population size using this method requires both pre- and post-bottleneck samples. Approaches that attempt to elucidate demographic history from a single genetic sample have therefore grown in popularity.

Correspondence: Joseph I. Hoffman, Fax: 0049 (0) 521 1062998; E-mail: joseph.hoffman@uni-bielefeld.de

Three classical single-sample methods for detecting population bottlenecks are the heterozygosity excess (Cornuet & Luikart 1996), mode-shift (Luikart *et al.* 1998) and *M*-ratio (Garza & Williamson 2001) tests. The first and arguably most widely used of these is based on the premise that rare alleles are rapidly lost during a bottleneck but their loss only weakly influences heterozygosity. This generates a transient excess of heterozygosity (lasting up to $4 \times N_e$ generations, where N_e is the bottleneck effective population size) relative to a population at equilibrium with an equivalent number of alleles. The second test (Luikart *et al.* 1998) measures the impact of the loss of rare alleles on the overall allele frequency distribution. The underlying rationale is that large, non-bottlenecked populations should have a high proportion of alleles at low frequency (<0.1), whereas alleles of intermediate frequency (e.g. 0.1–0.2) are expected to become more abundant after a severe bottleneck. Third, the *M*-ratio of Garza & Williamson (2001), defined as the ratio of the total number of alleles (k) to the allelic size range (r), may also be informative in respect of bottleneck history. This statistic exploits the fact that the loss of any allele during a bottleneck will reduce k, whereas only the loss of alleles at the extremes of the size range will reduce r. Consequently, k will tend to reduce more quickly than r in declining populations, leading to the expectation than M will be smaller in recently bottlenecked populations than in those at equilibrium.

Although the mode-shift test has not been extensively evaluated, heterozygosity excess and the *M*-ratio have both been shown to perform well at distinguishing bottlenecked from non-bottlenecked samples when applied to empirical datasets from species or populations with contrasting demographic histories (Cornuet & Luikart 1996; Spencer *et al.* 2000; Beebee & Rowe 2001; Garza & Williamson 2001). Furthermore, recent simulations suggest that these two measures may convey subtly different signals, the *M*-ratio for example being most likely to correctly identify a bottleneck when pre-bottleneck population size was large, the bottleneck lasted several generations or the population subsequently made a demographic recovery (Williamson-Natesan 2005). However, a major drawback of both approaches is that they require simplifying assumptions to be made about the mutational mechanism of the genetic markers employed. These assumptions if incorrect have the potential to strongly influence equilibrium values of both heterozygosity conditional upon allele number and *M* (Guinand & Scribner 2003; Williamson-Natesan 2005; Busch *et al.* 2007).

Fortunately, emerging analytical approaches drawing upon Bayesian methodologies provide a novel avenue for exploring demographic history independently of the bottleneck tests described above. For example, by implementing a flexible demographic model, Bayesian Skyline Plots (BSPs) allow changes in effective population size (N_e) over time to be deduced without the need for assumptions to be made about key demographic parameters (Drummond *et al.* 2005). Potentially even more powerful is Approximate Bayesian Computation (ABC), an approach that allows for selection of the optimal demographic/evolutionary history and associated parameters among a set of hypothesized models (Beaumont *et al.* 2002; Bertorelle *et al.* 2010). This is achieved by generating alternative simulated datasets based on assumptions about evolutionary and demographic parameters which are then compared to the observed data using summary statistics.

Surprisingly few studies have used ABC to infer the bottleneck histories of natural populations, and these have largely explored events occurring over time scales of thousands of years (Chan *et al.* 2006; Thornton & Andolfatto 2006), often using a combination of ancient and contemporary samples. However, many conservation biologists are more interested in the impact of relatively recent, anthropogenically induced bottlenecks. Moreover, the use of ancient samples has largely restricted studies to using mitochondrial DNA (mtDNA) sequences, whereas the inclusion of multiple unlinked nuclear markers such as microsatellites holds the potential to substantially improve analytical power (Chan *et al.* 2006; Chevalet & Nikolic 2010). Finally, previous studies have lacked detailed historical observations with which to parameterize bottleneck scenarios for evaluation within the ABC framework.

The Antarctic fur seal (*Arctocephalus gazella*) provides an excellent opportunity to explore the relative abilities of established and emerging analytical approaches to detect a recent historical bottleneck. This species occurs predominantly to the south of the Antarctic Convergence, with 97% of the extant population breeding on the island of South Georgia (Fig. 1, Boyd & Roberts 1993). Like most other members of the Arctocephalus genus, Antarctic fur seals were subject to uncontrolled exploitation for their fur and oil during the late eighteenth and nineteenth centuries. Uniquely however, many of the journals and logbooks of early explorers and sealing captains have been retained and scrutinized (see Table S1, Supporting information) allowing detailed reconstruction of the timing and extent of the demographic reduction (Fig. 2). Census data are similarly available with which to track the post-exploitation recovery of the population (see Table S2, Supporting information). Together, these historical records allow the *a priori* parameterization of a plausible demographic model that can be tested using ABC.

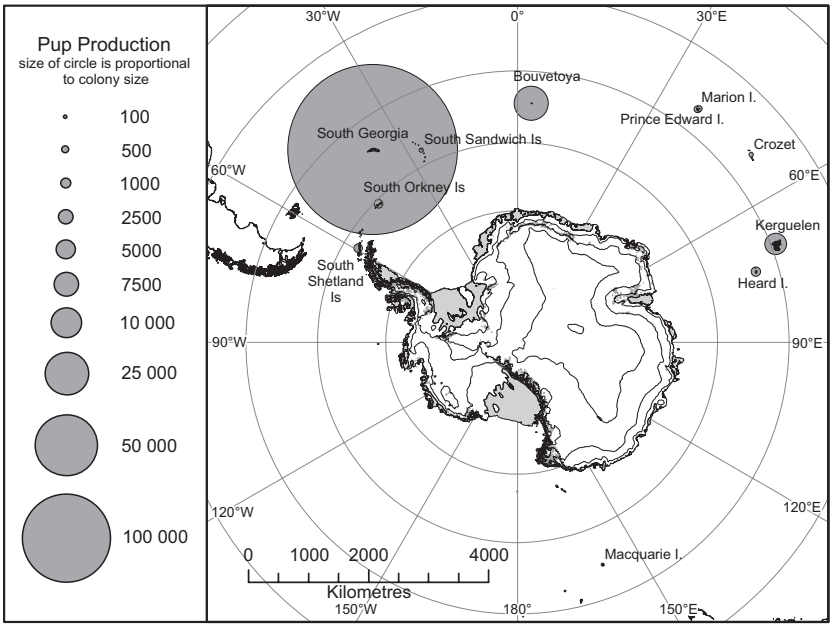

Fig. 1 Contemporary breeding distribution of the Antarctic fur seal. All of the named locations possess breeding colonies, with circle size being proportional to the pup production of each colony (see 'Introduction' for details). Modified from Forcada & Staniland (2009) with the permission of the authors.

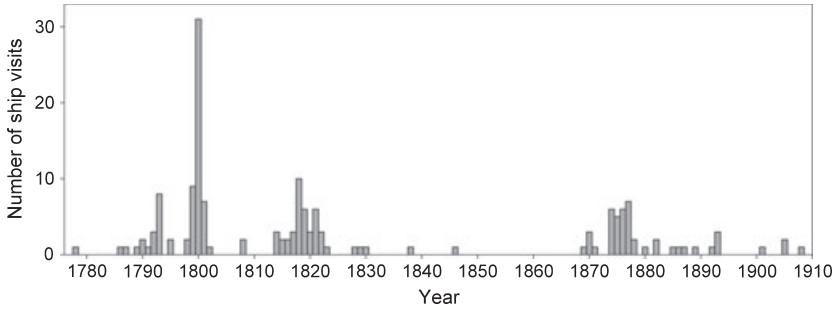

Fig. 2 The temporal distribution of fur sealing voyages to South Georgia reconstructed from historical sealing records (see Table S1 for the raw data). Annual numbers of sealing voyages were recorded together with the number of animals taken whenever this was known. However, because the catch size data are patchy and concerns have also been raised over their accuracy (Headland 1989), only the numbers of sealing trips are presented. As sealing seasons spanned the Southern Hemisphere summer, we refer to individual voyages by the year in which the ship was first recorded to have visited the sealing grounds. Ships that visited for a second season without returning home were recorded as separate voyages in consecutive years.

The exploitation of Antarctic fur seals began shortly after the discovery of South Georgia by Captain James Cook in 1775. The most profitable strategy was to take as many seals as it was possible to kill in one season, as Mill (1905) comments: 'Reckless extermination was the only method of seal-hunting resorted to on the islands of South Georgia and the coasts of South America so that the first in the field at a new sealing ground was sure of an immense booty, and late-comers as likely as not would go empty away'. Sealing at South Georgia reached its peak during the 1800–01 season (Fig. 2) with 31 ships recorded as having been operating there, 17 of which were responsible for a total catch of 112 000 seals (Fanning 1833). Such uncontrolled harvesting must have greatly depleted the population and probably explains the brief abatement of sealing activity that followed until a resurgence in 1814. By 1822, Weddell (1825) estimated that up to 1.2 million seals had been taken at South Georgia, and the almost-exterminated population was no longer able to sustain the industry.

After the last commercial catch of 170 fur seals in 1908, very few individuals were sighted until the 1950s. In 1915, a single juvenile male was found and immediately killed (Bonner 1964) and in 1911 Larsen (1920) also

reported sighting a group of 30 individuals. A dedicated fur seal survey found 38 animals at Bird Island in 1933 and inferred a total population of 60 (Bonner 1964). The Discovery expedition of 1936 subsequently reported 59 seals including 12 pups at the same location (Payne 1977), but the population is thought to have remained at around this level until the 1950s. Rapid population growth ensued in the 1960s and 1970s, and by 1990 fur seal numbers were estimated to have reached 1.5 million (Boyd 1993). The most recent estimate of 3 million was made at the XXIII Antarctic Treaty Consultative Meeting in 1999 (Specially Protected Species in Antarctica. XXIII ATCM/WP24. Agenda Item 7c; Meeting 1999).

Here, we genotyped 246 Antarctic fur seals from South Georgia at a 263-bp region of the hypervariable region 1 (HVR1) of the mitochondrial control region and 21 unlinked highly polymorphic microsatellites. Our aims were to explore the relative abilities of classical bottleneck tests and Bayesian approaches to recover a signal of historical exploitation and to estimate via ABC the distributions of key bottleneck parameters including timing and minimum population size. Our approach differs from previous studies using ABC in two main respects. First, our dataset comprises both mtDNA and microsatellite data, bringing enhanced genetic resolution as well as bi-parental perspectives. Second, population reduction resulting from harvesting and subsequent recovery are well documented in this species, providing a strong *a priori* demographic model.

Materials and methods

Tissue sample collection

Tissue samples were collected from Antarctic fur seal pups during the austral summer of 2003/2004 from an intensively studied colony at Bird Island where an elevated scaffold walkway (Doidge *et al.* 1984) provides access to animals with minimal disturbance. Additional samples were obtained from a neighbouring colony at Freshwater Beach on Bird Island, from the nearby Willis Islands and also from several rookeries around mainland South Georgia that were visited opportunistically by sailing boat (Table 1 and Fig. S1, Supporting information). Samples were taken from the fore-flipper using piglet ear-notching pliers and stored individually in the preservative buffer 20% dimethylsulphoxide (DMSO) saturated with salt at −20 °C.

DNA extraction and microsatellite genotyping

Total genomic DNA was extracted using an adapted Chelex 100 protocol and phenol-chloroform purified.

Table 1 Numbers of Antarctic fur seals genotyped at the mitochondrial HVR1 and 21 microsatellite loci. For a detailed map of the sampling locations, see Fig. S1 (Supporting information)

Location	Sampling site	Number of samples genotyped
Willis Islands	Main Island	16
Bird Island	Study colony	142
	Freshwater beach	25
Mainland	Prince Olav Harbour	12
South Georgia	Leith Harbour	1
	Husvik	12
	Cooper Bay	14
	Annenkov Island	15
	Wilson Harbour	9
		246

Each sample was then genotyped at 21 unlinked microsatellite loci (Table 2) as described in detail by Hoffman & Amos (2005). Loci were amplified using the following PCR profile: one cycle of 120 s at 94 °C, 45 s at T_1, 50 s at 72 °C; 10 cycles of 30 s at 94 °C, 45 s at T_1, 50 s at 72 °C; 25 cycles of 30 s at 89 °C, 45s at T_2, 50s at 72 °C; and one final cycle of five minutes at 72 °C (see Table 2 for T_1 and T_2). PCR products were resolved by electrophoresis on standard 6% polyacrylamide sequencing gels, detected by autoradiography and scored manually. GENEPOP (Raymond & Rousset 1995) was used to calculate observed and expected microsatellite heterozygosities and to test for deviations from Hardy–Weinberg equilibrium and for linkage disequilibrium. For each of these tests, we set the dememorization number to 10 000, the number of batches to 1000 and the number of iterations per batch to 10 000.

Mitochondrial DNA sequencing

A 316-bp region of the mitochondrial hypervariable region 1 (HVR1) was PCR amplified using Thr/Pro (5′-TCCCTAAGACTCAAGGAAGAG-3′) and Cent (5′-GAGCGAGAAGAGGTACACTTT-3′) following Wynen *et al.* (2000). Each PCR was carried out in a 25 μL reaction volume containing 10 ng of template DNA, 10 mM Tris–HCl (pH 8.3), 50 mM KCl, 2 mM $MgCl_2$, 0.1% Tween 20, 0.1% gelatine, 0.1% IGEPAL, 0.05 mM dNTPs, 0.4 μM of each primer and 0.25 units of *Taq* polymerase. The following PCR profile was used: one cycle of 120 s at 94 °C; 15 cycles of 45 s at 94 °C, 45s at 50 °C, 60 s at 72 °C; 25 cycles of 45 s at 90 °C, 45 s at 50 °C, 60 s at 72 °C; and one final cycle of 5 min at 72 °C. Ten microlitres of PCR product was purified using Antarctic phosphatase and exonuclease I (New England

Table 2 Details of the 21 microsatellite loci employed in this study and their polymorphism characteristics in 246 Antarctic fur seals

Locus	Isolated from species	Reference	T_1 (°C)	T_2 (°C)	Number of alleles	H_E	H_O	HWE P value
Aa4	South American fur seal *Arctocephalus australis*	Gemmell *et al.* (1997)	46	48	6	0.745	0.715	0.372
Ag10	Antarctic fur seal *Arctocephalus gazella*	Hoffman *et al.* (2008)	46	48	7	0.771	0.758	0.206
Agaz1	Antarctic fur seal *Arctocephalus gazella*	Hoffman (2009)	50	54	13	0.872	0.814	**0.010**
Agaz2	Antarctic fur seal *Arctocephalus gazella*	Hoffman (2009)	46	48	10	0.793	0.794	0.218
Hg1.3	Grey seal *Halichoerus grypus*	Gemmell *et al.* (1997)	42	46	13	0.871	0.855	0.920
Hg6.3	Grey seal *Halichoerus grypus*	Allen *et al.* (1995)	46	48	13	0.869	0.842	0.051
Hg6.10	Grey seal *Halichoerus grypus*	Allen *et al.* (1995)	55	60	14	0.850	0.884	0.595
Hg8.10	Grey seal *Halichoerus grypus*	Allen *et al.* (1995)	42	46	5	0.499	0.520	0.065
Lw8	Weddell seal *Leptonychotes weddellii*	Davis *et al.* (2002)	42	46	13	0.903	0.937	0.892
Lw10	Weddell seal *Leptonychotes weddellii*	Davis *et al.* (2002)	46	48	17	0.909	0.898	0.750
Lw15	Weddell seal *Leptonychotes weddellii*	Davis *et al.* (2002)	48	52	14	0.883	0.803	**0.008**
M11a	Southern elephant seal *Mirounga leonina*	Hoelzel *et al.* (1999)	46	48	18	0.918	0.906	0.353
OrrFCB1	Atlantic walrus *Odobenus rosmarus rosmarus*	Buchanan *et al.* (1998)	45	50	10	0.789	0.718	0.220
OrrFCB7	Atlantic walrus *Odobenus rosmarus rosmarus*	Buchanan *et al.* (1998)	55	60	12	0.851	0.865	0.720
OrrFCB8	Atlantic walrus *Odobenus rosmarus rosmarus*	Buchanan *et al.* (1998)	55	60	8	0.786	0.812	0.156
OrrFCB16	Atlantic walrus *Odobenus rosmarus rosmarus*	Buchanan *et al.* (1998)	55	60	4	0.578	0.615	0.128
Pv9	Grey seal *Halichoerus grypus*	Allen *et al.* (1995)	48	52	10	0.753	0.765	0.809
PvcA	Harbour seal *Phoca vitulina*	Coltman *et al.* (1996)	46	48	7	0.782	0.754	0.677
PvcE	Harbour seal *Phoca vitulina*	Coltman *et al.* (1996)	45	50	14	0.875	0.882	0.970
Zcwb07	Galapagos sea lion *Zalophus californianus wollebaeki*	Hoffman *et al.* (2007)	48	52	12	0.853	0.896	0.335
Zcwg04	Galapagos sea lion *Zalophus californianus wollebaeki*	Hoffman *et al.* (2007)	46	48	17	0.901	0.879	0.532

T_1 and T_2 denote PCR annealing temperatures. H_E, expected heterozygosity; H_O observed heterozygosity. Individually significant Hardy-Weinberg equilibrium (HWE) P values at $\alpha < 0.05$ are highlighted in bold. None of these remained significant following table-wide sequential Bonferroni adjustment.

Biolabs) following the manufacturer's recommended protocol. Samples were then sequenced using the Applied Biosystems BigDye® Terminator v3.1 Cycle Sequencing Kit and analysed on an ABI PRISM™ 377 DNA sequencer. Fragments were sequenced initially from the 5′-end, but were also repeated from the 3′-end if the first sequence was either too short or contained one or more ambiguous bases. Consensus sequences were generated using ChromasPro version 1.3.4 and all of the sequences were then aligned manually within BioEdit version 5.0.6 (Hall 1999). Sites containing insertions/deletions or missing data were removed, including a highly variable region enriched for TC repeats that was previously described by Wynen *et al.* (2000) as the 'TC landmark'. All the sequences were then trimmed to the length of the shortest sequence. This yielded 263-bp of contiguous sequence, corresponding to sites 14–292 of the Genbank sequence for Wynen *et al.*'s (2000) *A.gazella* haplotype 1 (AF384376). Finally, 17 randomly selected samples were repeated from scratch to determine repeatability. All the pairs of replicates were identical, suggesting that the mtDNA dataset is of high quality.

Tests for population substructure

Because the inference of historical changes in population size can be sensitive to population structure (Peter *et al.* 2010), we first checked for the presence of genetic subdivision within South Georgia by calculating pairwise F_{st} values among all of the sampling locations for both classes of marker. F_{st} was calculated for microsatellites using Fstat version 2.9.3 (Goudet 1995) and for mitochondrial DNA using Arlequin version 2.0 (Schneider *et al.* 2000). Mean pairwise F_{st} among populations was -2.5×10^{-5} (SE = 0.001, range = −0.011 to 0.012) for microsatellites and -0.032 (SE = 0.018, range = −0.367 to 0.105) for mtDNA. Only three of the 72 resulting values were individually significant at $P < 0.05$, none of which remained so following sequential Bonferroni correction for multiple tests. We also conducted a Bayesian cluster analysis of the microsatellite genotype dataset using the program Structure version 2.2.3 (Pritchard *et al.* 2000). This program uses a maximum likelihood approach to determine the most likely number of genetically distinct groups in a sample (K) by subdividing the dataset in a way that maximizes Hardy–Weinberg equilibrium and

linkage equilibrium within the resulting clusters. We ran five independent runs each for $K = 1$–9 using 1×10^6 MCMC iterations after a burn-in of 1×10^5, specifying the correlated allele frequencies model and assuming admixture. The replicate runs for each value of K were highly concordant for their output log likelihood values, with the highest values being consistently associated with $K = 1$ (Fig. S2, Supporting information), indicating a lack of genetic structure. Moreover, the results of subsequent data analyses were qualitatively similar regardless of whether the full dataset was used or analyses were restricted to the study colony at Bird Island (data not shown).

Microsatellite-based bottleneck tests

To test for evidence of a genetic bottleneck, we first used the heterozygosity excess method of Luikart *et al.* (1998) implemented within the program BOTTLENECK version 1.2.02 (Piry *et al.* 1999). One potential drawback of this approach is that, although microsatellites evolve mainly by gaining or losing a single repeat unit (the Stepwise Mutation Model, SMM (Kimura & Ohta 1978)), occasional larger 'jump' mutations of several repeat units are also common (Di Rienzo *et al.* 1994; Schlötterer *et al.* 1998). Consequently, BOTTLENECK allows the user to specify a range of mutation models, from the strict SMM through two-phase models (TPMs) with varying proportions of multi-step mutations to the infinite alleles model (IAM) where every new mutation is novel. For our analysis, four TPM models were evaluated with 1%, 5%, 10% and 30% multi-step mutations respectively and a default variance of 30. For each of the mutational models, the heterozygosity of each locus expected under mutation-drift equilibrium given the observed number of alleles (H_{eq}) was determined using 10 000 simulations and then compared against observed heterozygosity (H_e). We then recorded the number of loci for which H_e was greater than H_{eq} and determined whether the overall set of deviations was statistically significant using sign, standardized differences and Wilcoxon signed ranks tests. Bottlenecked populations are also expected to exhibit a characteristic 'mode shift' in the frequency distribution of alleles away from the L-shaped distribution expected under mutation-drift equilibrium (Luikart *et al.* 1998). Consequently, BOTTLENECK was also used to generate a qualitative descriptor of whether the observed allele frequencies at each locus deviate from such a distribution.

As an alternative test for a population bottleneck, we also calculated Garza and Williamson's M-ratio for our dataset using the program M_P_VAL (Garza & Williamson 2001). The significance of the resulting value was determined by comparison against a distribution of M values calculated from 10 000 theoretical populations in mutation-drift equilibrium. Using conventional criteria, a significant reduction in population size is inferred if fewer than 5% of the replicates fall below the observed value of M. The program allows the user to modify three parameters that approximate the mutation process in natural populations: the proportion of mutations that are larger than a single step (p_g), the average size of non-single-step mutations (Δ_g) and $\theta = 4\ N_e\mu$ (where N_e is the effective pre-bottleneck population size at equilibrium and μ is the mutation rate). We used the default settings of $p_g = 0.1$ and $\Delta_g = 3.5$, and varied θ between 1 and 1000, the latter corresponding to an effective pre-bottleneck population size of 500 000 assuming a commonly used estimate of the dinucleotide microsatellite mutation rate of 5×10^{-4} mutants per gamete per generation (Weber & Wong 1993) as suggested by Garza & Williamson (2001).

Mitochondrial DNA analyses

To visualize relationships among the observed mtDNA haplotypes, a median joining network was constructed within NETWORK version 4.516 (Bandelt *et al.* 1999). This program calculates all possible minimum spanning trees for the dataset and then combines these into a single minimum spanning network following an algorithm directly analogous to that proposed by Excoffier & Smouse (1994). Inferred intermediate haplotypes are then added to the network in order to minimize its overall length. For comparison, we also estimated a statistical parsimony network (Templeton *et al.* 1992) using the program TCS version 1.2.1 (Clement *et al.* 2000). This approach first defines the uncorrected distance between haplotypes above which the parsimony criterion is violated with more than 5% probability (the 'parsimony limit'). The haplotypes are then connected to one another, starting with those that are most similar, until either all of the haplotypes are included in a single network or the parsimony limit has been reached.

The distribution of the observed number of differences between each pair of haplotypes (the 'mismatch distribution', Slatkin & Hudson 1991; Rogers & Harpending 1992) was next calculated within ARLEQUIN. This typically forms a unimodal wave in samples drawn from recently expanded populations, whereas samples from static or bottlenecked populations tend to exhibit multimodal distributions (Slatkin & Hudson 1991; Rogers & Harpending 1992; Excoffier & Schneider 1999). ARLEQUIN was also used to calculate Harpending's raggedness index (Harpending 1994) and to test for deviation of the observed dataset from a model of rapid population expansion assuming the same mean number

of pairwise differences as the observed sample (Rogers & Harpending 1992). To test for deviations from neutrality, we also calculated Tajima's D (Tajima 1989) and Fu's F_s (Fu 1997) within ARLEQUIN. Significant negative values of these statistics indicate an excess of low frequency polymorphisms, a pattern commonly attributed to recent population expansion.

Bayesian skyline plot

MCMC sampling procedures (Drummond *et al.* 2005) were used to generate a BSP of female effective population size (N_{ef}) over time within BEAST version 1.5.4 (Drummond & Rambaut 2007). The Bayesian skyline algorithm describes a flexible demographic model which estimates the posterior distributions of theta ($\theta = N_{ef}\tau$, where τ = generation length) through time while minimizing assumptions about population growth trajectories. Three discrete changes in population size were allowed, a value selected so as not to over-parameterize the data. To allow derivation of N_{ef} from θ, we estimated τ, defined by Caswell (2001) as the mean age of mothers of the offspring produced by a cohort over its lifetime, at 9.89 years (SD = 2.42, range = 4.83–12.72) using 26 consecutive years of data within population models developed and implemented by Forcada *et al.* (2008).

Due to uncertainty over the exact HVR1 mutation rate, we explored a range of values. First, as a lower bound we used Dickerson *et al.*'s (2010) estimate of the HVR1 mutation rate of 5.74×10^{-7} substitutions per site per generation (s/s/gen) derived for *Callorhinus ursinus*. However, this may underestimate the true value because it was based on multiple species alignments, which represent more evolutionary time for recurrent mutation to occur among lineages. Second, we used Phillips *et al.*'s (2009) estimate of 2.71×10^{-6} s/s/gen derived for *Eumetopias jubatus*. This figure is potentially more realistic because it was obtained by calibration with a linked coding region, thereby correcting for homoplasies that would otherwise go undetected. Third, we estimated the rate directly for *A.gazella* based on mean pairwise sequence divergence from its sister taxon *A.tropicalis*, assuming a time to most recent common ancestor (t_{mrca}) of 20 thousand years ago (Higdon *et al.* 2007). The resulting value was unusually high at 3.65×10^{-5} s/s/gen and could quite possibly be a gross over-estimate due to uncertainty over Higdon *et al.*'s (2007) estimate of t_{mrca} at this shallow node. However, similarly high rates have also been reported over short time intervals in other species (Heyer *et al.* 2001; Subramanian *et al.* 2009). Consequently, we took the cautious approach of using this value as an upper bound for our analyses. Finally, we ran a fourth analysis making no prior assumptions on the mutation rate or t_{mrca}. Although this only generated relative parameter estimates that cannot be directly interpreted as actual N_{ef} or time, it allowed us to determine whether assumptions about the mutation rate or t_{mrca} affected the shape of the demographic reconstructions. All BSP analyses consisted of either 50 or 75 million MCMC iterations, depending on which of these produced acceptable effective sample sizes (ESS) as defined by the program authors for the posterior and prior distributions.

Approximate Bayesian Computation (ABC) analysis

Statistical support for alternative historical scenarios that either included or excluded a bottleneck was tested within an ABC framework. This allowed us not only to determine whether or not a bottleneck is likely to have occurred, but also to estimate values of key parameters of interest. We initially simulated two primary historical models. The first incorporated a recent population bottleneck, with prior distributions broadly surrounding values derived from historical records (Fig. 2). The model described an ancestral N_e uniformly distributed between 1 and 1.5×10^6, the upper bound encompassing Weddell's (1825) estimate of 1.2 million seals having been taken during the initial bout of harvesting. The occurrence of the bottleneck was described by two uniform distributions representing the time parameter associated with $N_{e\text{-}historical}$ (15–100 generations ago) and the time associated with the end of the bottleneck (i.e. with the lowest value of $N_{e\text{-}bottleneck}$, 1–30 generations ago). The bottleneck model was constrained such that changes in effective population size occur simultaneously. The prior on $N_{e\text{-}bottleneck}$ was bounded between 1 and 1000, values that generously surround the 1911 census population of 30 individuals (Larsen 1920). $N_{e\text{-}contemporary}$ was uniformly distributed between 1 and 1.5×10^6. For comparison, a null model of no population bottleneck was also defined, in which N_e was uniformly distributed through time (1–100 generations) and bounded between 1 and 1.5×10^6 individuals. For both models, the HVR1 mutation rate was defined by a uniform distribution with lower and upper bounds of 5.74×10^{-7} (Dickerson *et al.* 2010) and 2.71×10^{-6} (Phillips *et al.* 2009) s/s/gen respectively. The HKY + I + G (I = 0.57, G = 0.50) mutation model defined for HVR1 was determined using the hierarchical likelihood ratio test and Akaike information criterion, as implemented in JMODELTEST v 0.1.1 (Posada 2008). For microsatellites, the generalized stepwise mutation model (Estoup *et al.* 2002) was implemented with a mean rate uniformly distributed between 1.00×10^{-4} and 1.00×10^{-3} substitutions/generation. These simulations were performed assuming a 1:1 sex ratio.

To explore the influence of prior assumptions on posterior distributions using ABC we next initiated a series of simulations incorporating prior parameter adjustments. Specifically, we examined the influence of assumptions on the prior distributions of the mitochondrial mutation rate and sex ratio on the posterior distributions of parameters of interest. This was important because the assumed value of $\mu_{mitochondrial}$ describes the source of genetic diversity for simulated populations while sex ratio influences the diversity of bi-parentally inherited markers. The effect of HRV1 mutation rate prior was explored using a liberal prior bounded by 5.74×10^{-7} and 3.65×10^{-5} s/s/gen. The effect of assuming a 1:1 sex ratio was assessed through additional simulations based on a sex ratio of one male to five females. This sex ratio was drawn from field observations and it is unclear how accurately this value reflects the true genomic contributions of the two sexes.

In addition to the above simulations, all models were simulated a second time, but with broadened uniform priors on all parameters relating to N_e and time. Specifically, contemporary and historic N_e were distributed between 1 and 6×10^6, bottleneck N_e between 1 and 2000, time associated with $N_{e\text{-}historical}$ between 1 and 500 generations ago, and timing of the end of the bottleneck between 1 and 50 generations ago. Prior distributions of parameters for all analyses are described in Table 4. Finally, to assess whether the strength of the bottleneck signal differs between the mtDNA and microsatellite datasets, additional simulations were performed on each data type independently. These were carried out twice, once with the initially defined priors on N_e and time, and also following the broadened priors on these parameters.

For each model, one million genetic datasets were simulated with the defined demographic and marker parameters. Four summary statistics were then generated for the observed and simulated datasets: mean pairwise difference and Tajima's *D* (Tajima 1989) for HVR1, and mean heterozygosity and the mean number of alleles for microsatellites. Normalized Euclidean distances were calculated between the observed dataset and each of the simulated datasets using the local linear regression method of Beaumont *et al.* (2002). The ten thousand datasets with the smallest Euclidean distances were then retained to build posterior parameter distributions, which were smooth weighted using the Locfit function within R version 2.9.1 (R Development Team 2005). The posterior probabilities of each scenario were estimated using a logistic regression approach, providing both point estimates and 95% confidence intervals (Fagundes *et al.* 2007; Cornuet *et al.* 2008). Statistical measures of performance and Type I and Type II error rates were also calculated as a means of model checking (Excoffier *et al.* 2005). All the above analyses were implemented within the DIYABC v1 software package (Cornuet *et al.* 2008, 2010).

Results

To test for a genetic signature of a historical population bottleneck, we genotyped 246 Antarctic fur seals from nine rookeries across South Georgia (Table 1) at 21 microsatellite loci and sequenced a 263-bp segment of the hypervariable region 1 (HVR1) of the mitochondrial control region. The microsatellite loci were highly informative, possessing on average 11.3 alleles and with a mean observed heterozygosity of 0.81 (Table 2). Following sequential Bonferroni correction to compensate for multiple statistical tests, none of the loci deviated significantly from Hardy-Weinberg equilibrium and no pairs of loci exhibited significant linkage disequilibrium. The same was found restricting the dataset to the study colony on Bird Island (n = 142, Table S3, Supporting information). A total of 26 mitochondrial haplotypes were identified, eleven of which (Genbank accession numbers

Table 3 The number of loci with heterozygosity excess and test probabilities obtained using a range of mutational models (see 'Materials and methods' for details) within the program BOTTLENECK (Piry *et al.* 1999)

Mutational model	No. of loci with heterozygosity excess	Sign test *P* value	Standardized differences test *P* value	Wilcoxon test *P* value
IAM	21	**<0.0001**	**<0.0001**	**<0.0001**
TPM70	20	**<0.001**	**<0.0001**	**<0.0001**
TPM90	17	**0.008**	**0.002**	**<0.001**
TPM95	16	0.075	**0.018**	**0.008**
TPM99	16	0.076	0.326	0.320
SMM	12	0.531	0.373	0.919

The mode test revealed normal L-shaped distributions under all of the scenarios tested. *P* values significant at $\alpha < 0.05$ without correction for multiple statistical tests are highlighted in bold.

Table 4 Prior uniform distributions, mean, median, mode, quantiles and estimates of bias and precision (MRB = mean relative bias, RMSE = root mean square error) for the posteriors of parameters calculated from simulations of historic models that differed in prior bounds of specific parameters

Parameter	Model	Prior	Mean	Median	Mode	5%	95%	MRB	RMSE
$N_{e\text{-}contemporary}$	**Initial**	1–1.5 × 10^6	7.44 × 10^5	7.42 × 10^5	1.78 × 10^5	6.69 × 10^4	1.42 × 10^6	6.50	98.68
	Sex ratio = 1:5		7.44 × 10^5	7.45 × 10^5	2.24 × 10^5	7.53 × 10^4	1.42 × 10^6	2.36	18.19
	Broadened μ_{seq}		7.38 × 10^5	7.33 × 10^5	4.32 × 10^5	7.00 × 10^4	1.43 × 10^6	5.76	58.36
	Microsatellites only		7.45 × 10^5	7.44 × 10^5	1.94 × 10^5	7.28 × 10^4	1.42 × 10^6	4.49	40.78
	Broadened	1–6 × 10^6	2.98 × 10^6	2.97 × 10^6	6.98 × 10^5	2.79 × 10^5	5.72 × 10^6	2.13	11.90
	Sex ratio = 1:5		2.95 × 10^6	2.92 × 10^6	2.74 × 10^5	2.73 × 10^5	5.67 × 10^6	6.10	60.50
	Broadened μ_{seq}		3.01 × 10^6	3.04 × 10^6	5.17 × 10^6	2.85 × 10^5	5.71 × 10^6	7.80	105.60
	Microsatellites only		3.00 × 10^6	2.98 × 10^6	2.72 × 10^6	2.93 × 10^5	5.70 × 10^6	2.83	19.90
$N_{e\text{-}bottleneck}$	**Initial**	1–1000	164	139	122	46	371	0.62	1.85
	Sex ratio = 1:5		356	313	215	92	821	0.77	2.70
	Broadened μ_{seq}		169	140	133	48	429	0.60	2.69
	Microsatellites only		188	153	153	53	563	0.68	2.97
	Broadened	1–2000	658	662	688	217	1070	0.43	1.49
	Sex ratio = 1:5		1200	1250	1360	469	1810	0.48	3.64
	Broadened μ_{seq}		660	667	678	228	1090	0.42	1.30
	Microsatellites only		665	655	593	216	1100	0.33	0.98
$N_{e\text{-}historical}$	**Initial**	1–1.5 × 10^6	7.77 × 10^5	7.63 × 10^5	3.96 × 10^5	1.55 × 10^5	1.43 × 10^6	1.56	22.52
	Sex ratio = 1:5		3.60 × 10^5	2.42 × 10^5	1.17 × 10^5	6.39 × 10^4	1.10 × 10^6	3.29	33.13
	Broadened μ_{seq}		7.48 × 10^5	7.20 × 10^5	3.59 × 10^5	1.44 × 10^5	1.42 × 10^6	1.07	8.64
	Microsatellites only		6.31 × 10^5	5.94 × 10^5	9.56 × 10^3	1.19 × 10^4	1.41 × 10^6	2.90	35.65
	Broadened	1–6 × 10^6	2.41 × 10^6	2.05 × 10^6	7.40 × 10^5	3.20 × 10^5	5.49 × 10^6	0.83	3.52
	Sex ratio = 1:5		9.07 × 10^5	4.35 × 10^5	9.88 × 10^4	6.79 × 10^4	3.67 × 10^6	2.03	20.00
	Broadened μ_{seq}		2.29 × 10^6	1.92 × 10^6	5.74 × 10^5	2.87 × 10^5	5.42 × 10^6	1.31	6.57
	Microsatellites only		2.79 × 10^6	2.76 × 10^6	1.13 × 10^4	1.23 × 10^5	5.67 × 10^6	9.04	133.37
$\tau_{bottleneck\text{-}end}$	**Initial**	1–30	12	11	6	2	27	0.77	2.49
	Sex ratio = 1:5		13	12	6	2	27	0.75	2.31
	Broadened μ_{seq}		12	11	5	2	27	0.81	2.49
	Microsatellites only		13	12	7	3	28	1.05	2.87
	Broadened	1–50	17	13	5	2	42	0.97	3.08
	Sex ratio = 1:5		17	13	4	2	43	0.67	2.38
	Broadened μ_{seq}		17	13	7	2	43	1.00	3.56
	Microsatellites only		18	14	1	2	44	0.95	2.93
$\tau_{historical}$	**Initial**	15–100	70	74	100	32	98	0.18	0.59
	Sex ratio = 1:5		69	72	96	29	98	0.16	0.57
	Broadened μ_{seq}		71	74	99	32	98	0.14	0.56
	Microsatellites only		71	74	94	31	98	0.19	0.59
	Broadened	1–2000	316	329	490	104	485	2.5	17.88
	Sex ratio = 1:5		284	287	279	77	475	1.60	14.18
	Broadened μ_{seq}		316	327	466	105	484	3.62	3.56
	Microsatellites only		320	333	497	108	486	2.83	23.33

Table 4 (Continued)

Parameter	Model	Prior	Mean	Median	Mode	5%	95%	MRB	RMSE
$\mu_{mitochondrial}$	**Initial**	5.74×10^{-7}–2.71×10^{-6}	1.67×10^{-6}	1.67×10^{-6}	6.27×10^{-7}	6.80×10^{-7}	2.64×10^{-6}	0.20	0.61
	Sex ratio = 1:5		1.64×10^{-6}	1.65×10^{-6}	2.70×10^{-6}	6.43×10^{-7}	2.62×10^{-6}	0.15	0.58
	Broadened μ_{seq}		1.84×10^{-5}	1.84×10^{-5}	7.52×10^{-6}	2.37×10^{-6}	3.47×10^{-5}	0.98	3.14
	Broadened	5.74×10^{-7}–3.65×10^{-5}	1.65×10^{-6}	1.65×10^{-6}	5.78×10^{-7}	6.67×10^{-7}	2.65×10^{-6}	0.21	0.65
	Sex ratio = 1:5		1.57×10^{-6}	1.52×10^{-6}	5.78×10^{-7}	6.31×10^{-7}	2.65×10^{-6}	0.22	0.68
	Broadened μ_{seq}		1.85×10^{-5}	1.85×10^{-5}	1.21×10^{-6}	2.22×10^{-6}	3.47×10^{-5}	1.29	4.18
$\mu_{microsatellite}$	**Initial**	1.00×10^{-4}–1.00×10^{-3}	4.69×10^{-4}	4.31×10^{-4}	2.66×10^{-4}	1.34×10^{-4}	9.12×10^{-4}	0.29	0.92
	Sex ratio = 1:5		4.85×10^{-4}	4.53×10^{-4}	2.49×10^{-4}	1.35×10^{-4}	9.27×10^{-4}	0.26	0.84
	Broadened μ_{seq}		4.75×10^{-4}	4.35×10^{-4}	2.98×10^{-4}	1.35×10^{-4}	9.23×10^{-4}	0.33	0.93
	Microsatellites only		5.24×10^{-4}	5.00×10^{-4}	4.12×10^{-4}	1.56×10^{-4}	9.38×10^{-4}	0.32	0.91
	Broadened	1.00×10^{-4}–1.00×10^{-3}	3.16×10^{-4}	2.46×10^{-4}	1.44×10^{-4}	1.18×10^{-4}	7.68×10^{-4}	0.25	0.78
	Sex ratio = 1:5		3.90×10^{-4}	3.26×10^{-4}	1.78×10^{-4}	1.37×10^{-4}	8.61×10^{-4}	0.24	0.68
	Broadened μ_{seq}		3.12×10^{-4}	2.45×10^{-4}	1.38×10^{-4}	1.17×10^{-4}	7.59×10^{-4}	0.18	0.73
	Microsatellites only		3.53×10^{-4}	2.85×10^{-4}	1.83×10^{-4}	1.18×10^{-4}	8.17×10^{-4}	0.28	0.79

JF304904–JF304914) had not previously been described by Wynen *et al.* (2000).

Classical bottleneck tests

We first interrogated our microsatellite dataset for evidence of a genetic bottleneck using the heterozygosity excess approach of Luikart *et al.* (1998). The results were highly dependent on the mutational model upon which the predicted relationship between heterozygosity and the number of alleles was based (Table 3). Thus, a significant excess of heterozygosity relative to expectations was detected under the IAM but not the SMM and *P*-values obtained for TPM models scaled positively with the proportion of multi-step mutations specified. This pattern probably reflects the greater power of the IAM to detect a bottleneck (Cornuet & Luikart 1996), despite this model being unrealistic for most 'real' microsatellites (Di Rienzo *et al.* 1994). A mode shift in the allele frequency distribution was not detected.

Recent simulations (Williamson-Natesan 2005) suggest that when pre-bottleneck population size was large or the population made a demographic recovery, the ratio of the number of alleles to allelic size range may be more informative about bottleneck history than heterozygosity excess. Consequently, we also calculated the *M*-ratio of Garza & Williamson (2001). The resulting value of 0.798 lies above the 0.7 threshold proposed by Garza & Williamson (2001), implying a lack of support for a bottleneck. Comparing this value against a null distribution derived from 10 000 theoretical populations in mutation-drift equilibrium, a bottleneck signature was only inferred below $\theta = 1.63$, a value that corresponds to a pre-bottleneck N_e of 812 assuming a default microsatellite mutation rate of 5×10^{-4} (Weber & Wong 1993). This seems unrealistically low given Weddel's (1825) report of 1.2 million seals having been harvested.

Historical inference from mtDNA

For an alternative perspective on the recent demographic history of the species, we generated a Median Joining Network (MJN) and mismatch distribution. The MJN was remarkably diffuse, invoking the presence of 59 missing intermediate haplotypes (Fig. 3a). A qualitatively similar network was also obtained using statistical parsimony (data not shown), the main difference being that several of the more distantly connected haplotypes in the original MJN violated the parsimony limit and were thus no longer incorporated (illustrated by open circles in Fig. 3a). The observed mismatch distribution was multimodal (Fig. 3b, Harpending's raggedness index = 0.034, $P = 0.025$), allowing us to reject a

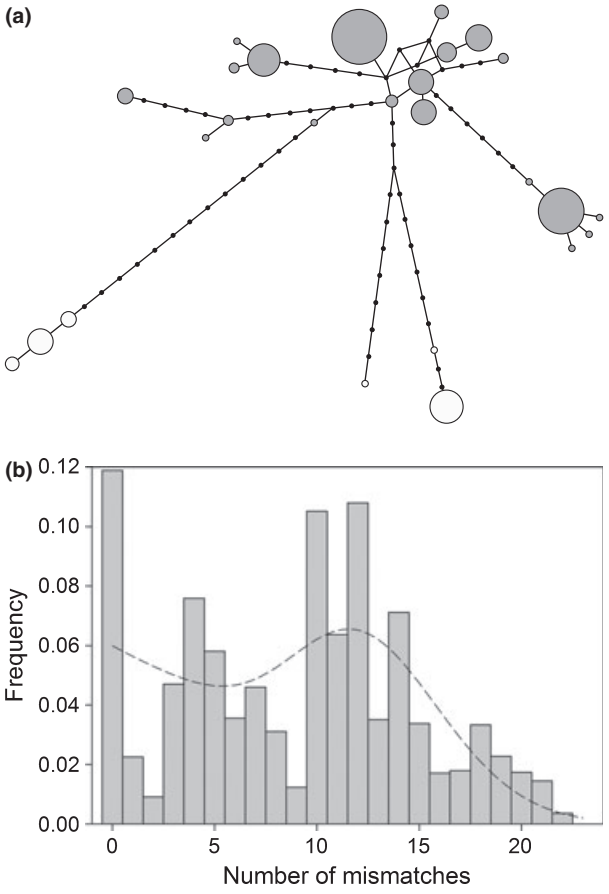

Fig. 3 Phylogenetic relationships among 26 mitochondrial HVR1 haplotypes observed in 246 Antarctic fur seals. (a) a median joining network in which each line joining two circles corresponds to a single nucleotide substitution, with grey circles representing observed haplotypes, black circles representing hypothetical haplotypes that were not observed in the sample and empty circles representing observed haplotypes that were not connected to the rest of the network using a statistical parsimony approach (see Materials and methods for details). Circle sizes reflect the relative frequency of each of the observed haplotypes. (b) histogram showing the observed distribution of pairwise differences. For comparison, the dashed line represents the expected distribution under a model of sudden population expansion.

model of historical population expansion. Moreover, Tajima's D (Tajima 1989) and Fu's F_s (Fu 1997) both rendered positive, non-significant values (D = 0.632, P = 0.801; F_s = 2.321, P = 0.774). Such a pattern is consistent with a genetic bottleneck but also cannot be readily distinguished from a static population at equilibrium (see 'Discussion').

Bayesian skyline plot

We next attempted to reconstruct a historical profile of female effective population size (N_{ef}) over time. Several

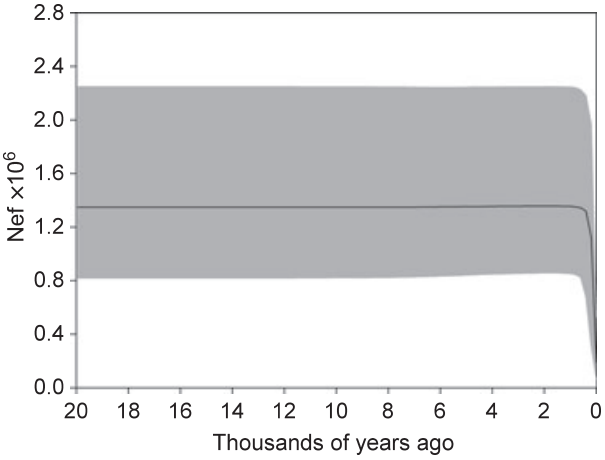

Fig. 4 Bayesian skyline plot displaying the median N_{ef} and 95% highest probability intervals plotted against time.

different Bayesian skyline analyses were conducted, each varying in prior constraints placed on coalescence time and mutation rate, but all generated consistently similar historical N_{ef} distributions. The emerging demographic pattern was one of a historically large and stable N_{ef} followed by a recent, sharp decline, the timing of which was not sensitive to prior assumptions on either μ or t_{mrca}. However, assumptions on μ did affect the magnitude of pre-bottleneck $N_{ef.}$ estimates. The BSP generated from the analysis with a 20kya coalescence time and a HVR1 mutation rate of 2.71×10^{-6} s/s/gen is shown in Fig. 4, as this yielded what we consider to be the most biologically plausible historical population size estimate (mean N_{ef} was estimated at 2.5 million for $\mu = 5.74 \times 10^{-7}$ s/s/gen, 1.4 million for $\mu = 2.71 \times 10^{-6}$ s/s/gen and 1800 for $\mu = 3.65 \times 10^{-5}$ s/s/gen).

Approximate Bayesian Computation (ABC) analysis

Evaluation of the two proposed historic models indicated that the one incorporating a population bottleneck based on historical observations most accurately described the genetic data. This model received a posterior probability of between 0.99 and 1, whereas the model depicting a constant population size through time received a posterior probability of between 0 and 0.01. In addition, Type I and Type II error rates for the selection of the bottleneck model were 0.18 and 0.12 respectively. The posterior distribution of selected parameters using values drawn from the 10 000 datasets closest to the observed are shown in Fig. 5 and Table 4. These indicate a genetic bottleneck that ended approximately 11 generations ago (mean = 12, median = 11, mode = 6 generations ago, 95% CI = 2–27) with an N_e at this time of approximately 139 (mean = 164, median = 139, mode = 122, 95% CI = 46–

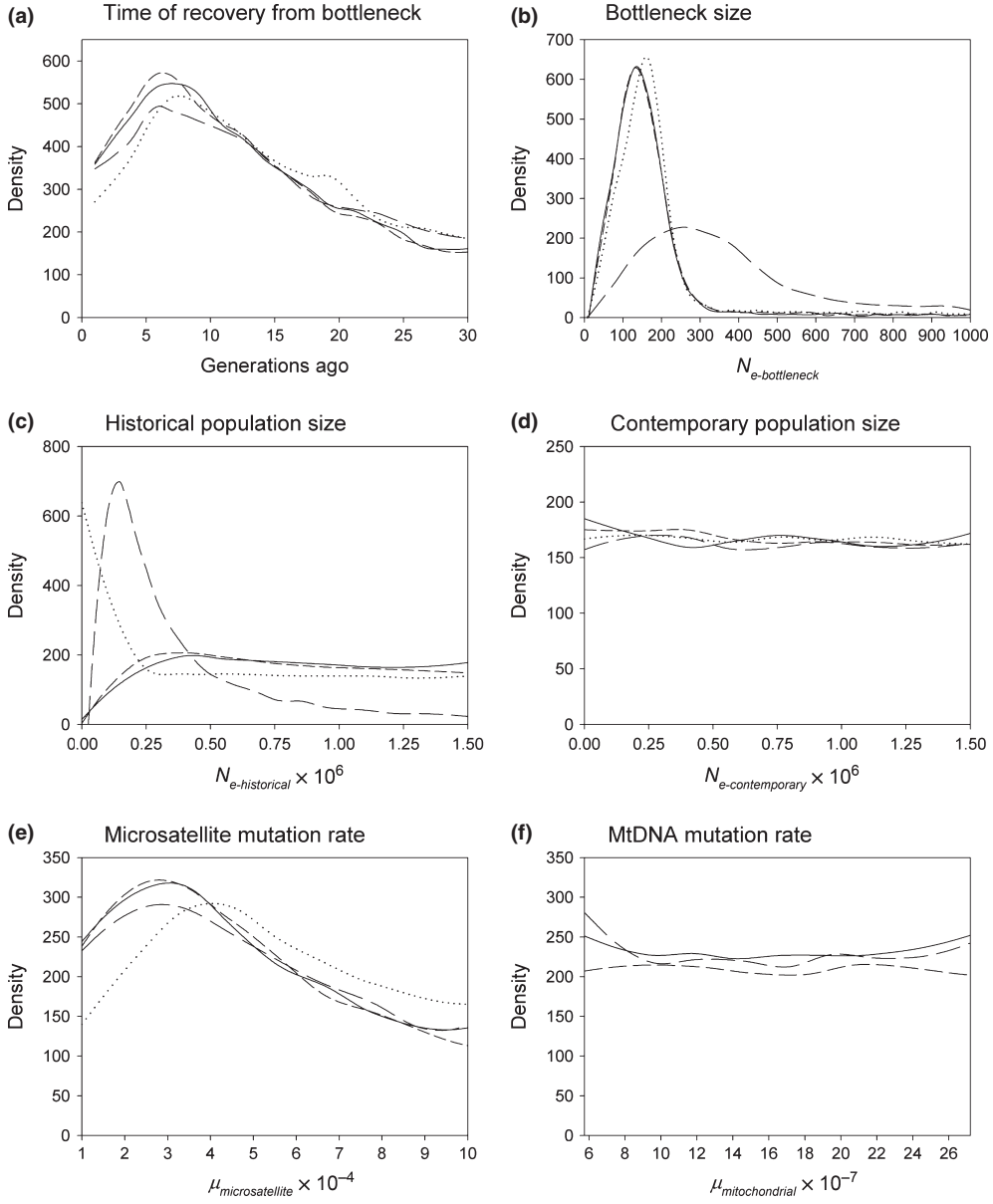

Fig. 5 Posterior density curves of model parameters based on 10 000 accepted values from 1×10^6 iterations of the initial bottleneck model (see 'Materials and methods' for details). Continuous, large-dashed and short-dashed lines represent posterior density curves obtained for simulations with a sex ratio of 1, a sex ratio of 1:5 and with expanded priors on mitochondrial mutation rate respectively. For the latter, data are only presented in panel f for the range 5.74×10^{-7} to 2.71×10^{-6}. Dotted lines represent results obtained for the microsatellite dataset only. Data from simulations using only mtDNA are not included due to the bottleneck model not being supported.

371). No clear posterior estimate of the time parameter associated with $N_{e\text{-historical}}$ was recovered (data not shown). The statistical descriptors for contemporary N_e were much larger (mean = 744 000, mean = 742 000, mode = 178 000, 95% CI = 66 900–1 420 000) and exhibited a flat posterior distribution. Estimates of historical N_e were also comparatively large (mean = 777 000, median = 763 000, mode = 396 000, 95% CI = 155 000–1 430 000), but the lower bound of the CI for historical N_e was over twice as large as that estimated for contemporary N_e. Moreover, the posterior distribution of historical N_e dipped towards lower N_e values indicating resolution for estimating the posterior lower bound of this parameter.

With Bayesian analytical approaches, choices of prior distributions can have a strong impact on posterior parameter estimates (Chan *et al.* 2006). Consequently, we explored the sensitivity of our analysis to a variety

of different prior assumptions (see 'Materials and methods' and Table 4 for details). Simulations involving prior parameter adjustments on sex ratio and mitochondrial mutation rate from the initial bottleneck model yielded largely unaltered estimates (Fig. 5, Table 4). The main deviation observed was in the estimation of bottleneck and historical N_e values from simulations invoking a 1:5 sex ratio. These analyses depicted a larger bottleneck N_e (about double the size) and a historical N_e peaking at around 0.2 million.

For our initial simulations, we chose prior distributions tightly bounded around values based on the available historical data. However, to explore sensitivity to these assumptions, we replicated all of the above simulations with wider priors on N_e and time (Fig. 6, Table 4). The bottleneck model was again highly sup-

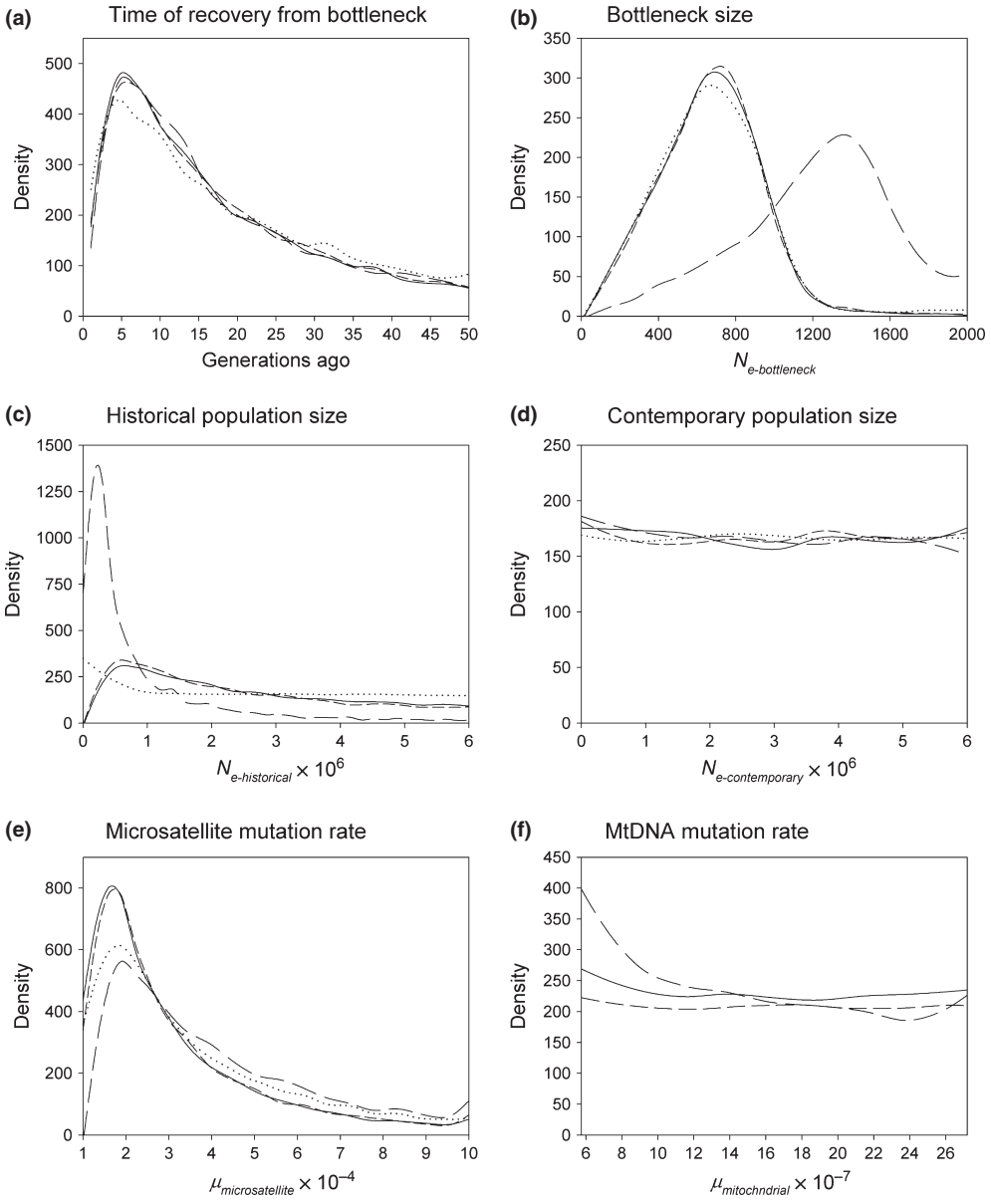

Fig. 6 Posterior density curves of model parameters based on 10 000 accepted values from 1×10^6 iterations of the bottleneck model with expanded priors on N_e and time (see 'Materials and methods' for details). Continuous, large-dashed and short-dashed lines represent posterior density curves obtained for simulations with a sex ratio of 1, a sex ratio of 1:5 and with expanded priors on mitochondrial mutation rate respectively. For the latter, data are only presented in panel f for the range 5.74×10^{-7} to 2.71×10^{-6}. Dotted lines represent results obtained for the microsatellite dataset only. Data from simulations using only mtDNA are not included due to the bottleneck model not being supported.

ported over the constant population size model (posterior probabilities were 1 and 0, respectively), with type I and II error rate estimates being lower than those obtained from the initial simulations (0.08 and 0, respectively). Parameter estimates were almost identical to those obtained in our initial simulations with the exception of bottleneck N_e, which was consistently larger at around 700 and 1400 for analyses based on a sex ratio of 1 and 1:5 respectively.

Finally, we tested for any potential differences in the strength of the bottleneck signal contained within the mtDNA and microsatellite datasets by conducting additional simulations separately for each class of marker. For microsatellites, the bottleneck model was supported over the constant population size model regardless of N_e and time priors (Figs 5 and 6; Table 4). Posterior support values were also closely comparable to those reported above (e.g. bottleneck model = 0.94–0.96 vs. constant population size model = 0.04–0.05 for simulations using the initial priors on N_e and time). In contrast, the mtDNA dataset was marginally better supported by the constant population size model than the bottleneck model (bottleneck model = 0.24–0.27; constant population size model = 0.72–0.75).

Discussion

Classical bottleneck tests are often used by conservation and evolutionary biologists to evaluate whether species have experienced historical demographic bottlenecks. In contrast, recently developed Bayesian approaches offer the potential to allow more detailed inferences in respect of both bottleneck timing and severity, but have not yet been thoroughly evaluated. Consequently, we analysed a multi-marker dataset using both sets of approaches to elucidate the possible impact of historical exploitation on Antarctic fur seals at South Georgia. Heterozygosity excess, mode-shift and *M*-ratio tests yielded unclear results. In contrast, Bayesian skyline and ABC analyses both yielded strong support for a recent and severe reduction in population size, with this inference appearing reasonably robust to a variety of prior assumptions.

Microsatellite-based tests for a bottleneck

Interpretation of the results of classical bottleneck tests was not straightforward. The heterozygosity excess approach yielded *P*-values that were highly dependent upon the underlying mutational model, a bottleneck being inferred using the IAM but not the SMM, despite the former being unrealistic for most microsatellites (Di Rienzo *et al.* 1994). We therefore explored a range of intermediate TPM models, these revealing evidence for a bottleneck only when the proportion of multi-step (non-SMM) mutations was greater than around 5%. The true proportion probably lies in the region of 10–15%, but can be highly variable among species, loci and even alleles (Garza & Williamson 2001; Ellegren 2004). Consequently, although our results are suggestive of a bottleneck, precise knowledge of the mutation mode of our markers would be needed to be sure. This uncertainty is further compounded by the results of the mode-shift and M-ratio tests, neither of which supported a bottleneck scenario.

Several other microsatellite-based studies of species thought to have experienced severe but temporary reductions in population size have either failed altogether to detect a bottleneck or, as with our study, yielded results that depend on the mutational model specified (Spong & Hellborg 2002; Waldick *et al.* 2002; Spear *et al.* 2006; Busch *et al.* 2007; Rosa de Oliveira *et al.* 2009). In at least some of these cases, too few markers may have been used to provide adequate resolution, a problem expected to disproportionately influence the more conservative SMM model. However, our study used 21 microsatellite loci, over twice the minimum number recommended by Luikart & Cornuet (1998). These loci were also highly informative, possessing on average 11.3 alleles (range = 5–18, Table 2). Finally, tests for heterozygosity excess applied to an independent dataset comprising 84 adult male individuals genotyped for a much larger panel of 76 microsatellite loci (Hoffman *et al.* 2010) yielded virtually identical results (data not shown).

A number of factors other than genetic resolution may also influence the strength and duration of a bottleneck signature. For example, immigration is capable of erasing a bottleneck signal within a few generations, particularly if the immigrants originate from a genetically divergent population, bringing with them rare alleles but not substantially affecting overall heterozygosity (Cornuet & Luikart 1996; Keller *et al.* 2001). Conversely, hybridization holds the potential to generate a false positive signal, for example, artificially lowering *M* by introducing gaps into the allele frequency distribution (Garza & Williamson 2001). Again however, neither of these are likely to be important in Antarctic fur seals. Global population structure is weak and much of the species' range is believed to have been seeded from South Georgia and not vice versa (Wynen *et al.* 2000), suggesting that historical immigration into our study area is likely to have been negligible. Similarly, although *A. gazella* is known to hybridize with the sub-Antarctic fur seal *A. tropicalis*, Wynen *et al.* (2000) found no shared haplotypes between these species and a sequence divergence of 8%, suggesting that this phenomenon is recent, not extensive and confined only to very small regions of range overlap.

One plausible explanation for the lack of a clear and pervasive bottleneck signal using classical tests draws upon the observation that this species recovered from the demographic reduction extremely rapidly, census sizes increasing from just a handful of individuals in the 1920s to around three million within fewer than ten generations of the recorded bottleneck. Rapid population expansion is expected to promote the recovery of allelic diversity (Slatkin & Hudson 1991) and will therefore tend to erode any pre-existing signal of heterozygosity excess (Cornuet & Luikart 1996). Similarly, given the unusually high average allelic richness of our panel of loci and assuming that most mutations are single-step, the majority of novel mutations would not be expected to broaden the allelic size range, and should therefore increase the *M*-ratio causing a corresponding reduction in significance.

Finally, another possible explanation for our results is that the bottleneck may not have been severe enough to generate a clear heterozygosity excess/M-ratio signal in the first place. However, this would require sufficiently large numbers of individuals to have escaped sealing, either at remote locations or perhaps even by shifting their range *en masse*, only to return after the departure of the sealers. The latter seems unlikely given the strong breeding site fidelity exhibited by both sexes (Hoffman *et al.* 2006) coupled with natal philopatry (Hoffman & Forcada, in review). Nevertheless, the Willis Islands provide a plausible refuge in the close vicinity of South Georgia that could potentially have sheltered a small breeding population (Wynen *et al.* 2000). To formally evaluate the scale of population reduction that could be detected in this species using classical bottleneck tests would require extensive simulations in order to account for key uncertainties including locus-specific mutation models and rates, and N_e values.

Inferences from the distribution of mitochondrial haplotypes

According to Rogers & Harpending (1992), populations that have undergone recent bottlenecks tend to exhibit ragged, multimodal mismatch distributions. This notion has received considerable empirical support (Excoffier & Schneider 1999; Weber *et al.* 2004; Johnson *et al.* 2007). For example, a recent study of the Guadalupe fur seal *Arctocephalus townsendi* that compared pre- with post-bottleneck samples recovered a unimodal distribution from the former but a multimodal distribution from the latter (Weber *et al.* 2004). Similarly, contemporary samples taken from three unexploited Antarctic phocid species reveal unimodal peaks indicative of Pleistocene expansion (Curtis *et al.* 2009) whereas the heavily exploited Juan Fernandez fur seal *A. philippii* shows a ragged distribution (Goldsworthy *et al.* 2000). Our study detected clear multimodality in the mismatch distribution of the Antarctic fur seal, which would appear consistent with the known recent history of the species. However, populations in demographic equilibrium are also expected to produce multimodal distributions, reflecting the highly stochastic nature of gene genealogies (Slatkin & Hudson 1991). Consequently, in our study the mismatch distribution is only informative if one is able to discount *a priori* the possibility of the population having remained at demographic equilibrium.

Another potential complication in interpreting the mismatch distribution relates to the presence of weak population structure across the species' range. Wynen *et al.* (2000) previously defined two mitochondrial clades, one associated with South Georgia, the South Shetlands, Bouvetøya and Marion Island, and a second encompassing the eastern populations of Iles Kerguelen and Macquarie Island. To test whether any of the distantly connected nodes within South Georgia's median joining network could have been sourced from the eastern clade, we constructed a second network incorporating populations sampled by Wynen *et al.* (2000) from across the species range (Fig. S3, Supporting information). Most of the haplotypes derived from the eastern region were absent from South Georgia, suggesting that they do not contribute appreciably to the overall topography of the South Georgia network. Nevertheless, these considerations highlight potential pitfalls in basing demographic inference entirely on contemporary mtDNA samples. A better understanding the mismatch distribution will have to await future studies that are able to incorporate range-wide, stratiographically positioned historical genetic samples.

Bayesian inference

In contrast to classical bottleneck tests and the mtDNA mismatch distribution, Bayesian skyline analysis provided clear evidence of a recent historical reduction in N_{ef}. This demographic trend was observed across BSPs generated from multiple analyses that differed in assumptions regarding t_{mrca} and μ, indicating the presence of a genetic signature within the observed data that is robust to variation in the assumptions of these parameters. Furthermore, the BSP's flexible demographic model was also able to detect a genetic signature of demographic decline despite the population having subsequently expanded. However, no signal of post-bottleneck recovery was observed, consistent with a similar lack of resolution for contemporary population size in our ABC analyses (see below).

By applying ABC methods to the full Antarctic fur seal genetic dataset comprising mtDNA sequence data

and 21 autosomal microsatellites, a bottleneck scenario defined using historical records was strongly supported over the alternative model of constant population size. Moreover, the parameters of the bottleneck model, being prior-bounded around harvest and post-harvest population data, retained posterior distributions that were highly consistent with the observational data. For example, the median estimate for the timing of the end of the genetic bottleneck returned from our initial model was 109 years ago (corresponding to the year 1894) with an associated median $N_{e\text{-}bottleneck}$ of 139 individuals. By comparison, the last commercial catch of fur seals took place in 1908 and the census size was shortly afterwards measured at 30 individuals (Larsen 1920). Such a remarkable degree of congruence between census and genetic estimates indicates a strong demographic signal for this historic event in the genetic dataset. Furthermore, although the posterior distribution of contemporary N_e was flat, suggesting the absence of a genetic signal for estimating this parameter, the distribution of pre-bottleneck N_e indicated relatively poor support for values below around 250 000. This is consistent with a historically large population that underwent a recent and drastic genetic bottleneck, after which N_e has potentially begun to recover. It may further indicate that the recency of the bottleneck has limited any signal present for describing contemporary N_e. Related, the observation that no clear posterior estimate of the time parameter associated with $N_{e\text{-}historical}$ was recovered from our analyses further suggests the erosion of this historic signal by the bottleneck.

Analytical sensitivity

A general area of uncertainty for many population genetic studies concerns assumptions on μ. In particular, t_{mrca}, which is required for calibrating the estimation of μ, is often unknown. Furthermore, perceived μ can also be highly dependent on the amount of evolutionary time represented in a given dataset (ranging from gametic and pedigree dataset rate estimates to those estimated over longer evolutionary time scales (Heyer *et al.* 2001; Phillips *et al.* 2009; Subramanian *et al.* 2009). To compensate for these sources of uncertainty, we constructed several alternative BSPs and also defined relatively broad prior distributions for $\mu_{mitochondrial}$ within the ABC framework. The BSPs recovered the same demographic trend regardless of $\mu_{mitochondrial}$, but pre-bottleneck N_{ef} estimates were found to scale negatively with μ. The relationship between these parameters is as would be expected under the coalescent given that phylogenetic relationships among haplotypes (and internode branch lengths) were approximately the same among analyses. In contrast, ABC analyses that differed in prior bounds of $\mu_{mitochondrial}$ (one analysis incorporating a prior on $\mu_{mitochondrial}$ that very broadly surrounded the prior for the other analysis) yielded highly congruent estimates for the parameters N_e and τ (particularly for the bottleneck itself) although neither produced a clear posterior definition of $\mu_{mitochondrial}$. By implication, $\mu_{mitochondrial}$ is not only difficult to estimate for this population history using ABC, but also appears to have little influence on posterior parameter distributions regardless of the exact scenario tested. This may be related to the fact that the bottleneck signal within ABC appears to be largely attributable to the microsatellite dataset (see below).

Parameter estimates obtained for simulations exploring sex ratio and prior boundaries on N_e and time were also in general highly congruent. Consequently, for simplicity we focused primarily on the results of the initial model, although summaries of all of the simulations are available in Table 4 and Figs 4 and 5. However, two important points of difference were observed. First, simulations invoking a 1:5 sex ratio yielded somewhat different estimates of $N_{e\text{-}bottleneck}$ and $N_{e\text{-}historical}$, with the former being roughly double that estimated through other simulations and the latter being approximately half the size. Second, simulations based on broadened prior definitions of N_e and time yielded $N_{e\text{-}bottleneck}$ estimates that were approximately four times larger than in our initial models. It is unclear which of these simulations lie closest to the truth. The prior bounds used for our initial simulations were appropriately bounded around values estimated from the available historical data, but could potentially have been too conservative in respect of historical and / or contemporary N_e. Similarly, although a sex ratio of 1:5 based on the numbers of adult males and females within the colony provides a reasonable upper bound for exploring the sensitivity of our analyses to variation in sex ratio, this figure is likely to be too extreme. Accurate estimation of the operational sex ratio is not yet possible for this species because this would require large numbers of complete male and female life histories incorporating individual-based measures of reproductive success and offspring survivorship. However, a limited molecular paternity analysis conducted previously at the same colony has shown that, despite Antarctic fur seals being moderately polygynous, appreciable numbers of females do not conceive to males sighted ashore, resulting in lower than expected levels of shared paternity (Hoffman *et al.* 2003).

Bottleneck severity

Although simulations incorporating a variety of prior distributions all independently supported a bottleneck model over one of constant population size and the

timing of recovery from the bottleneck was robustly defined, considerable latitude was observed in posterior estimates relating to N_e. This suggests that careful exploration of prior bounds is crucial to deriving realistic posterior estimates, particularly for historical and bottleneck population size, key parameters of interest to conservation biologists. By exploring a generous parameter space, we have shown that the true value of $N_{e\text{-}bottleneck}$ almost certainly lies above Larsen's (1920) census size of 30 individuals, and could be up to fifty times higher. Moreover, we can be fairly confident that the population remained small for only a few generations. Given that the substantial loss of genetic diversity is believed to require a prolonged period of very low population size (Amos & Harwood 1998), this may help to explain why the Antarctic fur seal remains one of the most genetically diverse of all pinniped species (Hoffman *et al.* 2009) despite having passed through a well-documented population bottleneck.

Contributions of different markers

We have been able to analyse a genetic dataset comprising more than one marker type thanks to a new framework that allows ABC to be implemented jointly for mtDNA and microsatellites (Cornuet *et al.* 2008). However, the question arises as to which of these two markers contributes most strongly to the detectable bottleneck signal. This could have an important bearing on the broader interpretation of our findings given that the classical bottleneck tests were based exclusively on microsatellites whereas only mtDNA was used for the mismatch and BSP analyses. It is not entirely clear *a priori* which of these two classes of marker would be expected to be most informative in respect of a bottleneck: mtDNA owing to its lower effective population size relative to the autosomal genome (Wilson *et al.* 1985) or microsatellites due to the enhanced resolution provided by 21 unlinked highly polymorphic loci (Chan *et al.* 2006). Our simulations incorporating only one data type support the latter, with the bottleneck model gaining strong support over a history of constant population size for the microsatellite dataset, but the constant population size model being marginally better supported for mtDNA. Moreover, posterior parameter estimates obtained when the analysis was restricted to microsatellites were also largely congruent with those based on the combined mtDNA and microsatellite data, the only exception being historical population size. This suggests that the failure of classical bottleneck tests to detect a clear bottleneck signal is more likely to be related to the underlying approach than to the microsatellite dataset being uninformative.

Conclusions

Although detailed historical records document a reduction in population size in the Antarctic fur seal down to 30 individuals or fewer, it seems likely that larger numbers may have escaped sealing, either by breeding at remote or inaccessible locations such as the Willis Islands (Wynen *et al.* 2000) or perhaps by remaining out at sea. Our results suggest that a dramatic reduction in population size did indeed take place, but that this may not have been substantial or long-lasting enough to have appreciably reduced levels of genetic diversity. Similar insights from other bottlenecked species offer to substantially improve our understanding of how historical demographic reductions influence contemporary genetic diversity, with important implications for the conservation and management of threatened natural populations.

Acknowledgements

We are extremely grateful to S. Poncet, D. Poncet, G. Robertson, C. Duck, E. Kraus and K. Cripps for collecting tissue samples from various sites around South Georgia, as well as D. Briggs, M. Jessop, K. Reid, R. Taylor, T. Walker and N. Warren for help with tissue sampling and logistical support at Bird Island. We also thank C. Garza for supplying us with an updated version of M_P_val, P. Fretwell for generating Fig. 1, R. Headland for advice on historical sealing records and K. Dasmahapatra and two anonymous referees for comments that helped improve the manuscript. This work was funded by a Natural Environment Research Council Strategic Alliance Fellowship awarded to JIH and a States of Jersey postgraduate scholarship awarded to SMG. Tissue samples were collected and retained under permits issued by the Department for Environment, Food and Rural Affairs and in accordance with the Convention on International Trade in Endangered Species of Wild Fauna and Flora. All field procedures were approved by the British Antarctic Survey (BAS). This work contributes to the BAS Dynamics and Management of Ocean Ecosystems (DYNAMOE) science programme.

References

Aars J, Ims RA, Liu HP *et al.* (1998) Bank voles in linear habitats show restricted gene flow as revealed by mitochondrial DNA (mtDNA). *Molecular Ecology*, **7**, 1383–1389.

Allen PJ, Amos W, Pomeroy PP, Twiss SD (1995) Microsatellite variation in grey seals (*Halichoerus grypus*) shows evidence of genetic differentiation between two British breeding colonies. *Molecular Ecology*, **4**, 653–662.

Amos W, Harwood J (1998) Factors affecting levels of genetic diversity in natural populations. *Philosophical Transactions of the Royal Society of London Series B-Biological Sciences*, **353**, 177–186.

Anderson EC, Williamson EG, Thompson EA (2000) Monte carlo evaluation of the likelihood for N_e from temporally spaced samples. *Genetics*, **156**, 2109–2118.

Bandelt H-J, Forster P, Rohl A (1999) Median-joining networks for inferring intraspecific phylogenies. *Molecular Biology and Evolution*, **16**, 37–48.

Beaumont MA (2003) Estimation of population growth or decline in genetically monitored populations. *Genetics*, **164**, 1139–1160.

Beaumont MA, Zhang W, Balding DJ (2002) Approximate Bayesian Computation in Population Genetics. *Genetics*, **162**, 2025–2035.

Beebee T, Rowe G (2001) Application of genetic bottleneck testing to the investigation of Amphibian declines: a case study with Natterjack Toads. *Conservation Biology*, **15**, 266–270.

Bertorelle G, Benazzo A, Mona S (2010) ABC as a flexible framework to estimate demography over space and time: some cons, many pros. *Molecular Ecology*, **19**, 2609–2625.

Bonner WN (1964) Population increase in the fur seal *Arctocephalus gazella* at South Georgia. In: Carrick R, Holdgate M, Prevost J (Eds) *Biologie Antarctique*. 1962, Hermann, Paris.

Boyd IL (1993) Pup production and distribution of breeding Antarctic fur seals (*Arctocephalus gazella*) at South Georgia. *Antarctic Science*, **5**, 17–24.

Boyd IL, Roberts JP (1993) Tooth growth in male Antarctic fur seals (*Arctocephalus gazella*) from South Georgia - an indicator of long-term growth history. *Journal of Zoology (London)*, **229**, 177–190.

Buchanan FC, Maiers LD, Thue TD *et al*. (1998) Microsatellites from the Atlantic walrus *Odobenus rosmarus rosmarus*. *Molecular Ecology*, **7**, 1083–1085.

Busch JD, Waser PM, DeWoody JA (2007) Recent demographic bottlenecks are not accompanied by a genetic signature in banner-tailed kangaroo rats (*Dipodomys spectabilis*). *Molecular Ecology*, **16**, 2450–2462.

Caswell H (2001) *Matrix Population Models*, 2nd edn. Sinauer Associates, Sunderland, Massachusetts.

Chan YL, Anderson CNK, Hadley EA (2006) Bayesian estimation of the timing and severity of a population bottleneck from ancient DNA. *PLoS Genetics*, **2**, e59.

Chevalet C, Nikolic N (2011) The distribution of coalescence times and distances between microsatellite alleles with changing effective population size. *Theoretical Population Biology*, **77**, 152–163.

Clement M, Posada D, Crandall KA (2000) TCS: a computer program to estimate gene genealogies. *Molecular Ecology*, **9**, 1657–1659.

Coltman DW, Bowen WD, Wright JM (1996) PCR primers for harbour seal (*Phoca vitulina concolour*) microsatellites amplify polymorphic loci in other pinniped species. *Molecular Ecology*, **5**, 161–163.

Cornuet JM, Luikart G (1996) Description and power analysis of two tests for detecting recent population bottlenecks from allele frequency data. *Genetics*, **144**, 2001–2014.

Cornuet JM, Santo F, Beaumont MA *et al*. (2008) Inferring population history with DIYABC: a user-friendly approach to Approximate Bayesian Computations. *Bioinformatics*, **24**, 2713–2719.

Cornuet JM, Ravign V, Estoup A (2010) Inference on population history and model checking using DNA sequence and microsatellite data with the software DIYABC (v1.0). *BMC Bioinformatics*, **11**, 401.

Curtis C, Stewart BS *et al*. (2009) Pleistocene population expansions of Antarctic seals. *Molecular Ecology*, **18**, 2112–2121.

Davis CS, Gelatt TS, Siniff D, Strobeck C (2002) Dinucleotide microsatellite markers from the Antarctic seals and their use in other pinnipeds. *Molecular Ecology Notes*, **2**, 203–208.

Di Rienzo A, Peterson AC, Garza JC *et al*. (1994) Mutational processes of simple sequence repeat loci in human populations. *Proceedings of the National Academy of Sciences, USA*, **91**, 3166–3170.

Dickerson BR, Ream RR, Vignieri SN, Bentzen P (2010) Population structure as revealed by mtDNA and microsatellites in Northern fur seals, *Callorhinus ursinus*, throughout their range. *PLoS ONE*, **5**, e10671.

Doidge DW, Croxall JP, Baker JR (1984) Density-dependent pup mortality in the Antarctic fur seal *Arctocephalus gazella* at South Georgia. *Journal of Zoology (London)*, **202**, 449–460.

Drummond AJ, Rambaut A (2007) BEAST: Bayesian evolutionary analysis by sampling trees. *BMC Evolutionary Biology*, **7**, 214.

Drummond AJ, Rambaut A, Shapiro B, Pybus OG (2005) Bayesian coalescent inference of past population dynamics from molecular sequences. *Molecular Biology and Evolution*, **22**, 1185–1192.

Ellegren H (2004) Microsatellites: simple sequences with complex evolution. *Nature Reviews Genetics*, **5**, 435–445.

Estoup A, Jarne P, Cornuet JM (2002) Homoplasy and mutation model at microsatellite loci and their consequences for population genetics analysis. *Molecular Ecology*, **11**, 1591–1604.

Excoffier L, Schneider S (1999) Why hunter-gatherer populations do not show signs of Pleistocene demographic expansions. *Proceedings of the National Academy of Sciences, USA*, **96**, 10597–10602.

Excoffier L, Smouse PE (1994) Using allele frequencies and geographic subdivision to reconstruct gene trees within a species: molecular variance parsimony. *Genetics*, **136**, 343–359.

Excoffier L, Estoup A, Cornuet JM (2005) Bayesian analysis of an admixture model with mutations and arbitrarily linked markers. *Genetics*, **169**, 1727–1738.

Fagundes NJR, Ray N, Beaumont MA *et al*. (2007) Statistical evaluation of alternative models of human evolution. *Proceedings of the National Acadamy of Sciences, USA*, **104**, 17614–17619.

Fanning E (1833) *Voyages and Discoveries in the South Seas 1792–1832*. Marine Research Society, Salem, Massachusetts.

Forcada J, Staniland IJ (2009) Antarctic fur seal *Arctocephalus gazella*. In: Perrin WF, Würsig B, Thewissen JGM (Eds) *Encyclopedia of Marine Mammals, 2nd Ed*. Academic Press (Elsevier).

Forcada J, Trathan PN, Murphy EJ (2008) Life history buffering in Antarctic mammals and birds against changing patterns of climate and environmental variation. *Global Change Biology*, **14**, 2473–2488.

Frankham R, Lees K, Montgomery M *et al*. (1999) Do population size bottlenecks reduce evolutionary potential? *Animal Conservation*, **2**, 255–260.

Fu YX (1997) Statistical tests of neutrality of mutations against population growth, hitchhiking and background selection. *Genetics*, **147**, 915–925.

Garza JC, Williamson EG (2001) Detection of reduced population size using data from microsatellite loci. *Molecular Ecology*, **10**, 305–318.

Gemmell NJ, Allen PJ, Goodman SJ, Reed JZ (1997) Interspecific microsatellite markers for the study of pinniped populations. *Molecular Ecology*, **6**, 661–666.

Goldsworthy S, Francis J, Boness D, Fleischer R (2000) Variation in the mitochondrial control region in the Juan Fernandez Fur Seal (*Arctocephalus philippi*). *Journal of Heredity*, **91**, 371–377.

Goudet J (1995) FSTAT (version 1.2): a computer program to calculate *F*-statistics. *Journal of Heredity*, **86**, 485–486.

Guinand B, Scribner KT (2003) Evaluation of methodology for detection of genetic bottlenecks: inferences from temporally replicated lake trout populations. *Comptus Rendus Biologies*, **326**, S61–S67.

Hall TA (1999) BioEdit: a user-friendly biological sequence alignment editor and analysis program for windows 95/98/NT. *Nucleic Acids Symposium Series*, **41**, 95–98.

Harpending H (1994) Signature of an ancient population growth in a low-resolution mitochondrial DNA mismatch distribution. *Human Biology*, **66**, 591–600.

Headland RK (1989) *Chronology of Antarctic Expeditions and Related Historical Events*. Cambridge University Press, Cambridge.

Hedrick PW, Miller PS (1992) Conservation genetics: techniques and fundamentals. *Ecological Applications*, **2**, 30–46.

Heyer E, Zietkiewicz E, Rochowski A *et al.* (2001) Phylogenetic and familial estimates of mitochondrial substitution rates: study of control region mutations in deep-rooting pedigrees. *American Journal of Human Genetics*, **69**, 11113–11126.

Higdon JW, Bininda-Edmonds ORP, Beck RMD, Ferguson SH (2007) Phylogeny and divergence of the pinnipeds (Carnivora: Mammalia) assessed using a multigene dataset. *BMC Evolutionary Biology*, **7**, 216.

Hoelzel AR, LeBoeuf BJ, Reiter J, Campagna C (1999) Alpha-male paternity in elephant seals. *Behavioral Ecology and Sociobiology*, **46**, 298–306.

Hoffman JI (2009) A panel of new microsatellite loci for genetic studies of Antarctic fur seals and other otariids. *Conservation Genetics*, **10**, 989–992.

Hoffman JI, Amos W (2005) Microsatellite genotyping errors: detection approaches, common sources and consequences for paternal exclusion. *Molecular Ecology*, **14**, 599–612.

Hoffman JI, Boyd IL, Amos W (2003) Male reproductive strategy and the importance of maternal status in the Antarctic fur seal *Arctocephalus gazella*. *Evolution*, **57**, 1917–1930.

Hoffman JI, Trathan PN, Amos W (2006) Genetic tagging reveals extreme site fidelity in territorial male Antarctic fur seals *Arctocephalus gazella*. *Molecular Ecology*, **15**, 3841–3847.

Hoffman JI, Steinfartz S, Wolf JBW (2007) Ten novel dinucleotide microsatellite loci cloned from the Galápagos sea lion (*Zalophus californianus wollebaeki)* are polymorphic in other pinniped species. *Moleular Ecology Notes*, **7**, 103–105.

Hoffman JI, Dasmahapatra KK, Nichols HJ (2008) Ten novel polymorphic dinucleotide microsatellite loci cloned from the Antarctic fur seal *Arctocephalus gazella*. *Molecular Ecology Resources*, **8**, 459–461.

Hoffman JI, Dasmahapatra KK, Amos W *et al.* (2009) Contrasting patterns of genetic diversity at three different genetic markers in a marine mammal metapopulation. *Molecular Ecology*, **18**, 2961–2978.

Hoffman JI, Forcada J, Amos W (2010) Exploring the mechanisms underlying a heterozygosity-fitnesss correlation for canine size in the Antarctic fur seal *Arctocephalus gazella*. *Journal of Heredity*, **101**, 539–552.

Johnson JA, Dunn PO, Bouzat JL (2007) Effects of recent population bottle necks on reconstructing the demographic history of prairie chickens. *Molecular Ecology*, **16**, 2203–2222.

Keller LF, Jeffery KJ, Arcese P *et al.* (2001) Immigration and the ephemerality of a natural population bottleneck: evidence from molecular markers. *Proceedings of the Royal Society of London Series B-Biological Sciences*, **268**, 1387–1394.

Kimura M, Ohta T (1978) Stepwise mutation model and distribution of allelic frequencies in a finite population. *Proceedings of the National Academy of Sciences of the United States of America*, **75**, 2868–2872.

Lande R (1994) Risk of population extinction from fixation of new deleterious mutations. *Evolution*, **48**, 1460–1469.

Larsen CA (1920) Report of the Interdepartmental Committee on Research and Development in the Dependencies of the Falkland Islands, p. 657. His Majesty's Stationary Office, London.

Luikart G, Cornuet JM (1998) Empirical evaluation of a test for identifying recently bottlenecked populations from allele frequency data. *Conservation Biology*, **12**, 228–237.

Luikart G, Allendorf FW, Cornuet JM, Sherwin WB (1998) Distortion of allele frequency distributions provides a test for recent population bottlenecks. *Journal of Heredity*, **89**, 238–247.

Luikart G, Cornuet JM, Allendorf FW (1999) Temporal changes in allele frequencies provide estimates of population bottleneck size. *Conservation Biology*, **13**, 523–530.

Lynch M, Conery J, Burger R (1995) Mutation accumulation and the extinction of small populations. *American Naturalist*, **146**, 489–518.

Mill HR (1905) *The Siege of the South Pole: The Story of Antarctic Exploration*. Alston Rivers, London.

Mills LS, Smouse PE (1994) Demographic consequences of inbreeding in remnant populations. *American Naturalist*, **144**, 412–431.

Payne MR (1977) Growth of a fur seal population. *Philosophical Transactions of the Royal Society of London, B*, **279**, 67–79.

Peter BM, Wegmann D, Excoffier L (2010) Distinguishing between population bottleneck and population subdivision by a bayesian model choice procedure. *Molecular Ecology*, **19**, 4648–4660.

Phillips CD, Trujillo RG, Gelatt TS *et al.* (2009) Assessing substitution patterns, rates and homoplasy at HVRI of Steller sea lions, *Eumetopias jubatus*. *Molecular Ecology*, **18**, 3379–3393.

Piry S, Luikart G, Cornuet J-M (1999) BOTTLENECK: a computer program for detecting recent reductions in the effective population size using allele frequency data. *Journal of Heredity*, **90**, 502–503.

Posada D (2008) jModelTest: Phylogenetic Model Averaging. *Molecular Biology and Evolution*, **25**, 1253–1256.

Pritchard JK, Stephens M, Donnelly P (2000) Inference of population structure using multilocus genotype data. *Genetics*, **155**, 945–959.

R Development Team (2005) *R: A Language and Environment for Statistical Computing*. R Foundation for Statistical Computing, Vienna, Austria.

Raymond M, Rousset F (1995) Genepop (Version 1.2) - population genetics software for exact tests of ecumenicism. *Journal of Heredity*, **86**, 248–249.

Richards C, Leberg PL (1996) Temporal changes in allele frequencies and a population's history of severe bottlenecks. *Conservation Biology*, **10**, 832–839.

Rogers AR, Harpending H (1992) Population growth makes waves in the distribution of pairwise genetic differences. *Molecular Biology and Evolution*, **9**, 552–569.

Rosa de Oliveira L, Meyer D, Hoffman JI, Majluf P, Morgante JS (2009) Evidence of a genetic bottleneck in an El Nino affected population of South American fur seals, *Arctocephalus australis*. *Journal of the Marine Biological Association of the United Kingdom*, **89**, 1717–1725.

Schlötterer C, Ritter R, Harr B, Brem G (1998) High mutation rate of a long microsatellite allele in *Drosophila melanogaster* provides evidence for allele-specific mutation rates. *Molecular Biology and Evolution*, **15**, 1269–1274.

Schneider S, Roessli D, Excoffier L (2000) *ARLEQUIN ver 2.000: a software for population genetics data analysis*. Genetics and Biometry Laboratory, Department of Anthropology and Ecology, University of Geneva, Geneva, Switzerland.

Slatkin M, Hudson RR (1991) Pairwise comparisons of mitochondrial DNA sequences in stable and exponentially growing populations. *Genetics*, **129**, 555–562.

Spear SF, Peterson CR, Matocq MD, Storfer A (2006) Molecular evidence for historical and recent population size reductions of tiger salamanders (*Ambystoma tigrinum*) in Yellowstone National Park. *Conservation Genetics*, **7**, 605–611.

Spencer CC, Neigel JE, Leberg PL (2000) Experimental evaluation of the usefulness of microsatellite DNA for detecting demographic bottlenecks. *Molecular Ecology*, **9**, 1517–1528.

Spong G, Hellborg L (2002) A near-extinction event in lynx: do microsatellite data tell the tale? *Conservation Ecology*, **6**, 1–8.

Subramanian S, Denver DR, Millar CD *et al.* (2009) High mitogenomic evolutionary rates and time dependency. *Trends in Genetics*, **25**, 482–486.

Tajima F (1989) Statistical method for testing the neutral mutation hypothesisby DNA polymorphism. *Genetics*, **123**, 585–595.

Templeton AR, Crandall KA, Sing CF (1992) A cladistic analysis of phenotypic associations with haplotypes inferred from restriction endonuclease mapping and DNA sequence data. III. Cladogram estimation. *Genetics*, **132**, 619–633.

Thornton K, Andolfatto P (2006) Approximate Bayesian Inference reveals evidence for a recent, severe bottleneck in a Netherlands population of *Drosophila melanogaster*. *Genetics*, **172**, 1607–1619.

Waldick RC, Kraus S, Brown M, White BN (2002) Evaluating the effects of historic bottleneck events: an assessment of microsatellite variability in the endangered, North Atlantic right whale. *Molecular Ecology*, **11**, 2241–2249.

Waples RS (1989) A generalised approach for estimating effective population size from temporal changes in allele frequency. *Genetics*, **121**, 379–391.

Weber JL, Wong C (1993) Mutation of human short tandem repeats. *Human Molecular Genetics*, **2**, 1123–1128.

Weber DS, Stewart BS *et al.* (2004) Genetic consequences of a severe population bottleneck in the Guadalupe fur seal (*Arctocephalus townsendi*). *Journal of Heredity*, **95**, 144–153.

Weddell J (1825) *A voyage Towards the South Pole Performed in the Years 1822–1824*. Longman, Hurst, Rees, Orme, Brown and Green, London.

Williamson EG, Slatkin M (1999) Using maximum likelihood to estimate population size from temporal changes in allele frequencies. *Genetics*, **152**, 755–761.

Williamson-Natesan EG (2005) Comparison of methods for detecting bottlenecks from mirosatellite loci. *Conservation Genetics*, **6**, 551–562.

Wilson AC, Cann RL, Carr SM *et al.* (1985) Mitochondrial DNA and two perspectives on evolutionary genetics. *Biological Journal of the Linnean Sociey*, **26**, 375–400.

Wynen LP, Goldsworthy SD, Guinet C *et al.* (2000) Postsealing genetic variation and population structure of two species of fur seal (*Arctocephalus gazella* and *A. tropicalis*). *Molecular Ecology*, **9**, 299–314.

Data accessibility

DNA sequences: Genbank accessions JF304904-JF304914.

Sample locations and microsatellite data: DRYAD entry doi: 10.5061/dryad.0kj5n.

Supporting information

Additional supporting information may be found in the online version of this article.

Fig. S1 Map of South Georgia showing the locations from which 246 individual Antarctic fur seals were tissue-sampled.

Fig. S2 Results of the Structure (Pritchard *et al.* 2000) analysis, showing mean ± SE ln *P(D)* values based on five replicates for each value of *K*, the hypothesised number of groups in the data.

Fig. S3 A median joining network illustrating phylogenetic relationships among 39 mitochondrial HVR1 haplotypes observed in 371 Antarctic fur seals.

Table S1 Summary of sealing voyages to South Georgia including the names of ships and catches taken where known, together with literature sources

Table S2 Summary of post-bottleneck population sizes for the Antarctic fur seal population at South Georgia

Table S3 Polymorphism characteristics of 21 microsatellite loci in 142 Antarctic fur seals from the study colony at Bird Island, South Georgia

Please note: Wiley-Blackwell are not responsible for the content or functionality of any supporting information supplied by the authors. Any queries (other than missing material) should be directed to the corresponding author for the article.